

## Feasibility Study on Thermal Management System Using Two-phase Fluid Flow for Laser Type Space Solar Power System

Makiko ANDO<sup>1</sup>, Haruhiko OHTA<sup>1</sup>, Atsushi OKAMOTO<sup>2</sup> and Haruo KAWASAKI<sup>2</sup>

<sup>1</sup> Kyushu University, Fukuoka, Japan, ohta@aero.kyushu-u.ac.jp

<sup>2</sup> Japan Aerospace Exploration Agency, Tsukuba, Japan, okamoto.atsushi@jaxa.jp

### Abstract

In recent years, feasibility of Space Solar Power System (SSPS) was examined from various aspects. Thermal management of SSPS is one of the most serious problems because of the generation of a great amount of waste heat at high heat flux density for both systems of microwave SSPS and laser SSPS. Removal and transportation of such waste heat can be realized by using two-phase fluid flow for thermal management system of SSPS. Two-phase fluid flow is a promising method to transport a large amount of thermal energy because it accompanies the transportation of latent heat of vaporization. To realize the cooling of the laser medium, heat flux at the cooling surface should be lower than the critical heat flux determined by the fluid and flow conditions. Also, temperature of the system should be maintained at allowable level. The paper studies the feasibility for thermal management system of bulk laser type SSPS simulating the cooling process by two-phase fluid flow of water and FC72. To increase the critical heat flux on a large heat transfer surface, a new structure of narrow channel is devised and its performance is tested.

### 1. Introduction

Space Solar Power System (SSPS) is proposed as an alternative to the existing terrestrial power plants using fossil fuel or nuclear power. In recent years, feasibility of SSPS was examined from various aspects. There are two different types of SSPS. One is microwave SSPS where electric power is generated by solar cells and transmitted by microwave, and the other is laser SSPS where power of sunray is directly converted to laser power to be transmitted. Laser SSPS has advantage of high power conversion efficiency and of its simple system compared to microwave SSPS. Thermal management for both types of SSPS, however, becomes a serious problem due to the generation of a great amount of waste heat at high heat flux density as a result of power conversion loss.

The feasibility of thermal management system of microwave SSPS was examined for 10MW class model<sup>(1)</sup>, which was proposed in fiscal year 2003 for the extensive feasibility study for SSPS in Japanese group. The power satellite consists of a light condensing units with concave mirrors and lens. A lot of generator/transmitter unified modules are assembled to make one satellite, and radiators are located at the satellite periphery. Large amount of thermal energy dissipated from the generators is to

be removed and transported to the radiators by two-phase flow loops. In the analysis, water and FC72 were selected as working fluids. According to the analysis, the application of boiling and two-phase flow could realize the thermal management system for microwave SSPS, but it requires huge dimensions and launch mass. Furthermore, feasibility for the microwave SSPS is doubtful for a satellite of 1GW model, i.e. a standard capacity for future commercial systems. An enlarged circular satellite is impossible because huge amount of heat generated in the central part of the satellite cannot be successfully transported. There are two possible solutions for this problem. If the magnification of sunlight condensing is increased, the satellite diameter is reduced inversely

Table 1 Assumptions for CHF calculation

Working fluid	Water, FC72
Channel height	$s=5-50\text{mm}$
Channel length	$L=30-1000\text{mm}$
Mass velocity	$G=50-400\text{kg/m}^2\text{s}$
Saturation Temperature	$T_{\text{sat}}=0-200^\circ\text{C}$

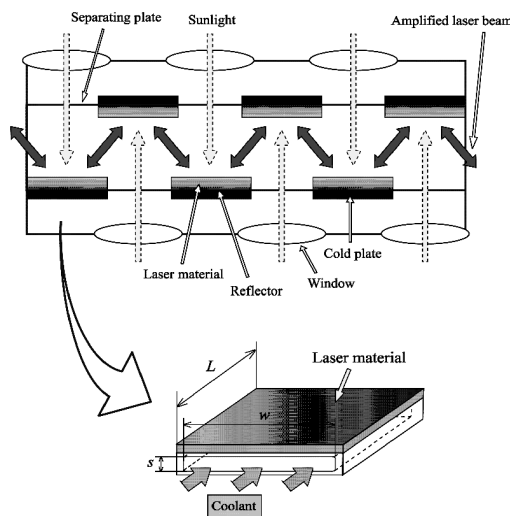


Fig. 1 Bulk laser type SSPS with active mirror laser amplification system.

proportional to the square root of the magnitude, while heat flux from generators is increased in proportion to the magnitude. To apply this idea it is essential to develop technologies to realize heat transfer at high heat flux from a large cold plate area. The other possibility is to separate the 1GW power satellite in several segments and to realize an assembly of ten 100MW class satellites. The system weight and volume is, however, seriously increased in both cases.

On the other hand, fiber laser type SSPS is proposed as a candidate of laser SSPS, which has advantage to minimize the dimension of satellite compared to that for microwave SSPS, and to reduce the size of the cooling system. The fiber laser type SSPS consists of the fiber bundles where sunray is converted to laser power and its energy is transmitted to earth or to other satellites. To enhance the power of sunray enough to excite the laser power, the sunray is condensed by a mirror. A fiber is composed of a core rod and a clad surrounding the core. By the difference of optical indices between them, the sunray is introduced to the fiber core through the clad. Generated laser power from one fiber is 1kW, for example, and the amount of 2kW is dissipated as thermal energy. To remove the waste heat, the clad is surrounded by a concentric fluid jacket with annular cross section. The two-phase system is again applied to reduce the liquid inventory and pump power. The waste heat is transported to the condensing section located at the opposite end of fiber bundles and radiated. Working

fluids are saturated water and FC72. In the past research, the heat transfer characteristics in boiling and two-phase flow is evaluated by correlations developed by authors<sup>(2)</sup> based on the boiling experiments under microgravity conditions. Radial temperature distributions across the fiber core and the clad were calculated. According to the calculated radial temperature distribution, temperature difference required for boiling heat transfer is estimated to be 10K at most. On the other hand, the temperature difference due to thermal conduction across the core and the clad requires much higher, and the selection of thick clad cannot maintain the fiber core temperature at low levels<sup>(3)</sup>.

The paper describes the simulation for the cooling process of bulk laser type SSPS using two-phase system. The possibility of cooling by two-phase fluid flow is discussed in terms of critical heat flux and temperature distribution in the laser medium.

### 2. Model of Bulk Laser Type SSPS

Bulk laser is one candidate of the laser SSPS. The cooling of a bulk piece of laser medium can be realized by the fluid flow in the rectangular channels located behind the laser medium. Figure 1 shows an example for the structure of bulk laser type SSPS. The present analysis is performed under the following assumptions; the magnification of sunray is more than 250, the conversion efficiency from sunray to laser power is 20-30%, thickness of the laser medium is 10mm, and uniform heat flux 250kW/m<sup>2</sup> is generated from the entire cooling

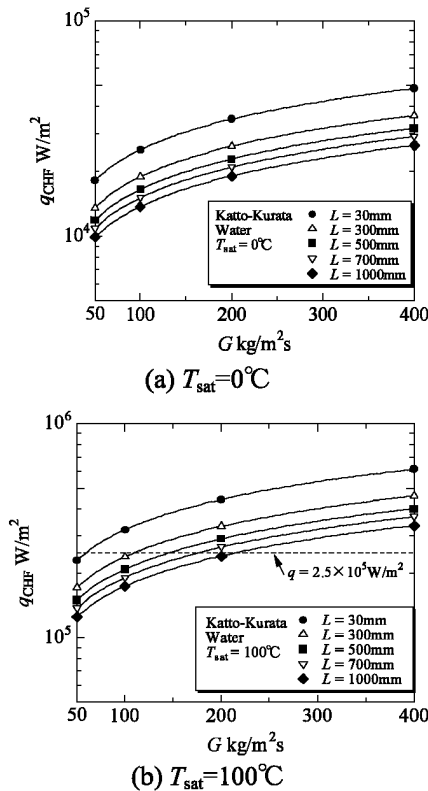


Fig. 2 Effect of mass velocity on critical heat flux (water).

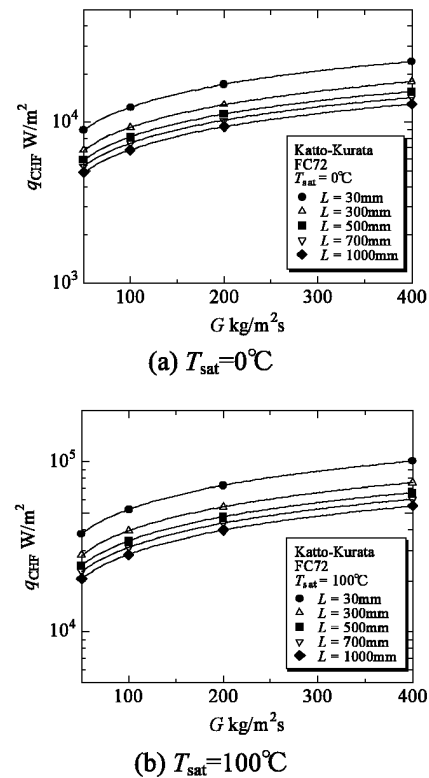


Fig. 3 Effect of mass velocity on critical heat flux (FC72).

surface of the laser medium. The heat flux is evaluated under assumptions of sunray magnification of 250 and conversion efficiency of 30%. In such a system, heat flux on the cooling surface of the medium should be lower than the critical heat flux determined by the flow conditions and channel dimensions. A state of saturated liquid at the inlet of the rectangular channel is assumed in the present analysis, and critical heat flux (CHF) is calculated by Katto-Kurata<sup>(4)</sup> and Mishima-Ishii<sup>(5)</sup> correlations developed for flow boiling in narrow channels on ground. Because there is no database or reliable correlation for the prediction of CHF in microgravity flow boiling in narrow channels, these correlations are employed in the present feasibility study to clarify the outline of cooling. Values of CHF are evaluated for water and FC72 under the conditions shown in Table 1.

Katto-Kurata correlation

$$\frac{q_{CHF}}{Gh_{fg}} = 0.186 \left( \frac{\rho_g}{\rho_l} \right)^{0.559} \left( \frac{\sigma \rho_l}{G^2 L} \right)^{0.264} \quad (1)$$

Mishima-Ishii correlation

$$q_{CHF} = \frac{A_{ch}}{A_h} h_{fg} \left[ \frac{G \Delta h_{sub,in}}{h_{fg}} + \left( \frac{1}{C_0} - 0.11 \right) \sqrt{\rho_g g (\rho_l - \rho_g) d_e} \right]$$

$$C_0 = 1.35 - 0.35 \sqrt{\rho_g / \rho_l}$$

$$d_e = 4 \times (\text{cross section}) / (\text{heated perimeter}) \quad (2)$$

where  $q_{CHF}$ : critical heat flux in  $W/m^2$ ,  $G$ : mass velocity in  $kg/m^2s$ ,  $h_{fg}$ : latent heat of vaporization in  $J/kg$ ,  $\rho_l$ : density of liquid in  $kg/m^3$ ,  $\rho_g$ : density of vapor in  $kg/m^3$ ,  $\sigma$ : surface tension in  $N/m$ ,  $L$ : channel length in  $m$ ,  $A_{ch}$ : channel cross-sectional area in  $m^2$ ,  $A_h$ : heated area in  $m^2$ ,  $\Delta h_{sub,in}$ : inlet subcooling in  $J/kg$ , and  $g$ : gravitational acceleration in  $m/s^2$ . The former correlation includes no effect of channel height, and the latter includes no effect of mass velocity when liquid is saturated at the inlet. It should be noted that these correlations are developed under the normal gravity condition, and configuration or size of the narrow channel system are different from those for the above correlations.

### 3. Calculated Results of CHF

Values of CHF are estimated based on the correlations mentioned in the previous section for the variation of channel height, heated length, fluid, mass velocity and saturation temperature. The following was obtained from the analysis.

i) Figures 2 and 3 show the effect of mass velocity on CHF by Katto-Kurata correlation for water and FC72, respectively. As is expected beforehand, CHF increases with increase in mass velocity and/or saturation temperature. On the other hand, CHF decreases with increase in heated length. There exist conditions that satisfy  $q_{CHF} > 250kW/m^2$  for water. In

the case of  $T_{sat}=100^\circ C$ , e.g.  $q_{CHF}$  is higher than  $250kW/m^2$  in the range of  $G > 140kg/m^2s$  when heated length is 500mm. When FC72 is used, however,  $q_{CHF}$  is lower than  $250kW/m^2$  in the range

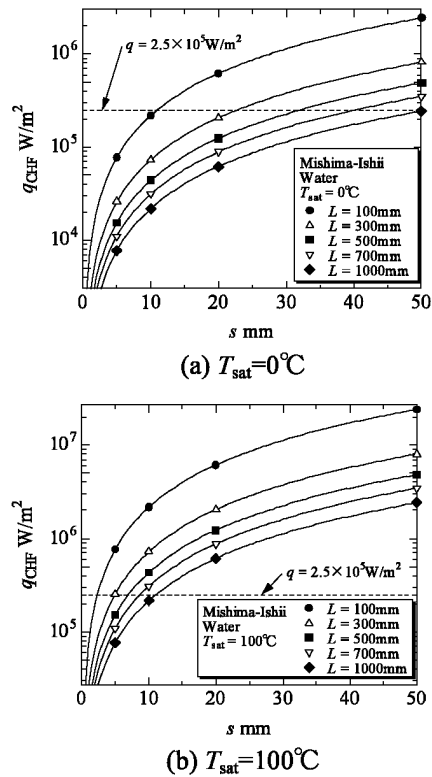


Fig. 4 Effect of channel height on critical heat flux (water).

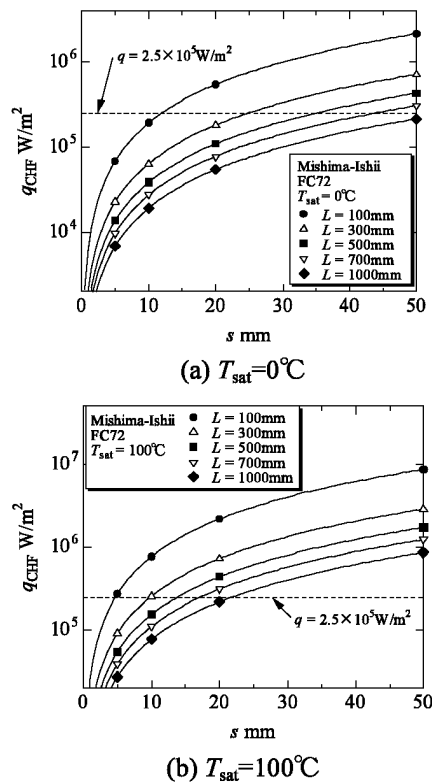


Fig. 5 Effect of channel height on critical heat flux (FC72).

of the present analysis mainly due to low values of latent heat of vaporization. Cooling by FC72 is impossible.

ii) The effect of channel height on CHF by Mishima-Ishii correlation is shown in Figures 4 and 5 for water and FC72, respectively. CHF increases with increase in channel height.

iii) Figures 6 and 7 show the relationship between CHF and heated length in the case of  $G=200\text{kg/m}^2\text{s}$  and  $s=20\text{mm}$ , respectively. The results are shown only for water because the cooling by FC72 is impossible according to, at least, the evaluation by Katto-Kurata correlation as already indicated in Fig.3. CHF decreases with increase in heated length but seems to be more sensitive to saturation temperature.

iv) Since CHF values in microgravity could be lower than those estimated in the present analysis, the range in the possible selection of channel dimensions and flow conditions are more restricted.

**4. Temperature Distribution in Laser Medium**

To examine the feasibility of thermal management by the present cooling model, the temperature distribution in the laser medium should be discussed. Figure 8 shows the schematic of temperature distribution in the laser medium. The laser medium temperature takes a maximum value  $T_s$  at the surface where laser beam enters, and  $T_s$  is expressed as

$$T_s = T_{\text{sat}} + \Delta T_{\text{conv}} + \Delta T_{\text{cond}} \tag{3}$$

where  $\Delta T_{\text{conv}}$  is the temperature difference required

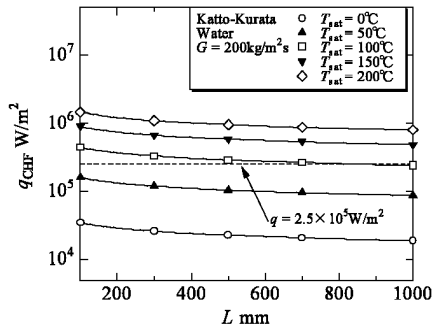


Fig. 6 Effect of heated length on critical heat flux by Katto-Kurata correlation (water).

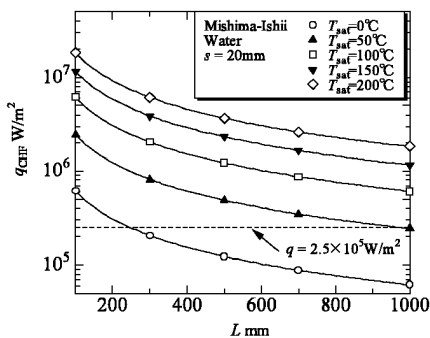


Fig. 7 Effect of heated length on critical heat flux by Mishima-Ishii correlation (water).

for the heat transfer by two-phase fluid flow, and  $\Delta T_{\text{cond}}$  is the temperature difference due to thermal conduction across the laser medium. The temperature  $T_s$  should be kept at lower value than the maximum allowable temperature of the laser medium. It is easily known from the studies of fiber laser SSPS,  $\Delta T_{\text{conv}}$  can be estimated in general as 30-40K at the highest, and  $\Delta T_{\text{cond}}$  varies depending on the kind of laser material and its thickness. Assuming that all of the generated heat is removed from the cooling surface of the laser medium,  $\Delta T_{\text{cond}}$  is given by

$$\Delta T_{\text{cond}} = \frac{\dot{q}}{2k} \delta^2 = \frac{q}{\delta} \frac{\delta^2}{2k} = \frac{q\delta}{2k} \tag{4}$$

where  $\dot{q}$ : rate of heat generation per unit volume in  $\text{W/m}^3$ ,  $q$ : heat flux on the cooling surface in  $\text{W/m}^2$ ,  $\delta$ : thickness of the laser medium in m and  $k$ : thermal conductivity of the laser medium in  $\text{W/mK}$ .

Figure 9 shows the temperature difference due to thermal conduction across the laser medium for the variation of thermal conductivity and thickness of the laser medium. The calculation was performed under the condition of  $q=250\text{kW/m}^2$ . Even at  $k=3\text{W/mK}$ , i.e. a value 30 times as large as that of glass,  $\Delta T_{\text{cond}}$  becomes higher than 400K for  $\delta=10\text{mm}$ . Since the maximum temperature of the laser medium  $T_s$  is the summation of  $T_{\text{sat}}$ ,  $\Delta T_{\text{conv}}$  and  $\Delta T_{\text{cond}}$ ,  $T_s$  takes much higher value than the maximum allowable temperature of the laser medium. As known from eq.(4),  $\Delta T_{\text{cond}}$  is proportional to heat flux  $q$  on the cooling surface and thickness  $\delta$  of the laser medium, and is inversely proportional to

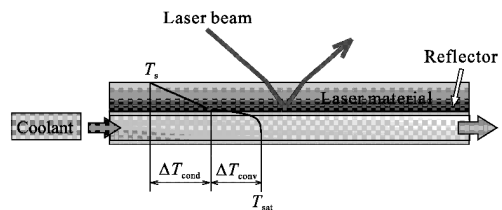


Fig. 8 Temperature distribution in the cooling of laser medium.

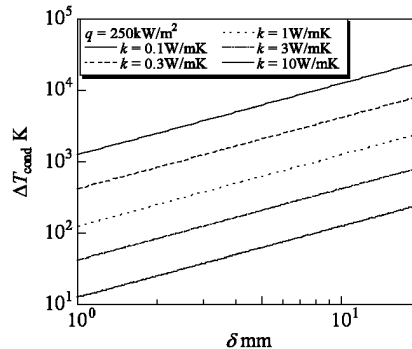


Fig. 9 Temperature difference due to thermal conduction across laser medium for different values of thermal conductivity and thickness.

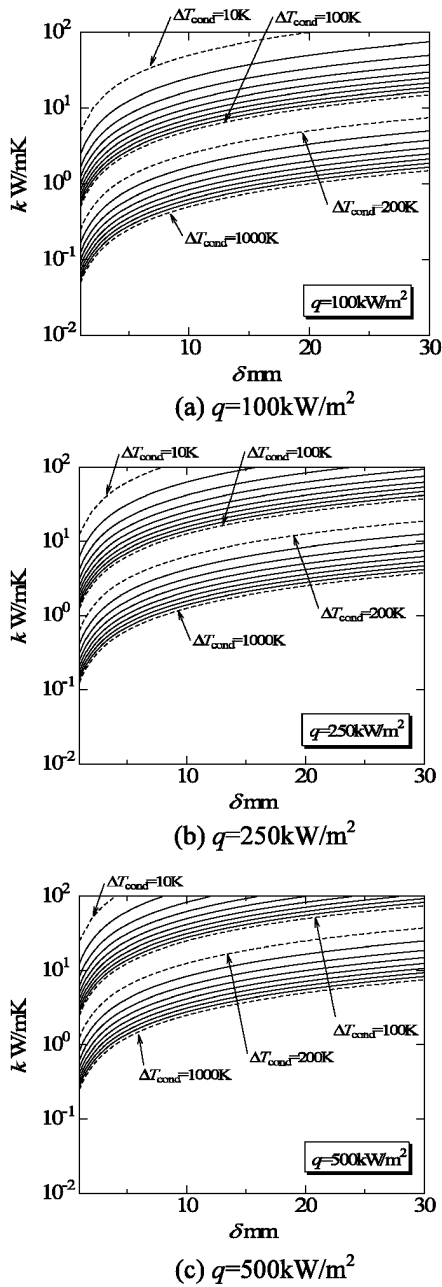


Fig. 10 Temperature difference in laser medium for the combination of thermal conductivity and thickness of laser medium.

thermal conductivity  $k$  of the laser medium. Therefore, it is necessary to reduce heat flux or thickness of the laser medium, or to use laser material of higher thermal conductivity to maintain temperature of the laser medium at lower levels.

Figure 10 shows the temperature difference  $\Delta T_{\text{cond}}$  across the laser medium by eq.(4) for the combinations of thermal conductivity and thickness of the laser medium at  $q=100, 250$  and  $500 \text{ kW/m}^2$ . Assuming that  $\Delta T_{\text{conv}}$  is about 30K, the temperature of working fluid  $T_{\text{sat}}$  is maintained at  $70^\circ\text{C}$ , and maximum temperature limitation of laser medium is  $150\text{-}200^\circ\text{C}$ , estimated maximum allowable value of  $\Delta T_{\text{cond}}$  becomes 50-100K. Even by using the laser

medium which has quite high thermal conductivity  $k=10 \text{ W/mK}$ , thickness of the laser medium should be less than 8.0mm to keep the laser medium temperature lower than  $200^\circ\text{C}$  for  $q=250 \text{ kW/m}^2$ . On the other hand, if heat flux at the cooling surface decreases to  $q=100 \text{ kW/m}^2$ , the laser medium could be thickened up to 20mm.

### 5. Devised Narrow Channels

As mentioned above, high heat flux cooling from a large area is inevitable to realize SSPS. To increase CHF for flow boiling in rectangular narrow channels, a method of liquid supply is devised to prevent dryout which is easily occurs in the downstream region under such cooling conditions. The structure of experimental apparatus is shown in Figure 11. The test section assembly has two narrow rectangular channels, i.e., a main heated channel and an auxiliary unheated channel located behind the main heated channel. The structure prevents burnout by the aid of enhanced liquid supply from an auxiliary unheated channel. The liquid is supplied additionally via sintered metal porous plates located at both sides of the main heated channel. Because the liquid is supplied additionally in the transverse direction perpendicular to the flow in the main heated channel, the structure reduces substantially the heated length to a half width of the present segment channel. Heating surface has arrays of groove to supply liquid to the center of the heating surface from the side of individual segment channels. The liquid flow is spontaneously induced by the capillary pressure difference when flattened bubbles cover the heating surface squeezing the liquid-vapor interface in the grooves. Experiments are performed under the following conditions; a size of heating surface:  $150 \text{ mmL} \times 30 \text{ mmW}$ , gap sizes of main heated channel:  $s=2 \text{ mm}$  and  $5 \text{ mm}$ , a gap size of auxiliary channel: 10mm, shape of grooves on the heating surface: 90 deg in apex angle and 1mm in pitch, test fluid: distilled water at 0.13MPa, inlet liquid velocity:  $u_{\text{in,main}}=0.065 \text{ m/s-} 0.2 \text{ m/s}$  (upward flow), inlet liquid subcooling:  $\Delta T_{\text{sub}}=15 \text{ K}$ , and the inlet velocity or mass velocity for the auxiliary unheated channel is reduced systematically by 2/3 and 1/3 of the values for the main heated channel.

Figure 12 shows the relation between values of CHF at downstream-center location (distance of 125mm from the upstream heating edge as shown in Fig.11) and total volumetric flow rate of liquid supplied to both channels for all experimental conditions. The following was obtained from the experiments.

i) In the case of the same total volumetric flow rate,

values of CHF for gap size of  $s=5\text{mm}$  are higher by around 1.5 times than those for gap size of  $s=2\text{mm}$ .

ii) CHF values larger than  $1 \times 10^6 \text{W/m}^2$  are obtained for all flow rates at  $s=5\text{mm}$  and for flow rates larger than  $2\text{l/min}$  at  $s=2\text{mm}$ .

iii) The values of CHF are quite insensitive to the reduction in the inlet liquid flow rate for the auxiliary channel. In other words, the same values of CHF are realized by smaller total flow rate of liquid.

iv) In the case of reduced inlet velocity for the auxiliary unheated channel, i.e.  $u_{in,aux} = (1/3)u_{in,main}$ , CHF values larger than  $1 \times 10^6 \text{W/m}^2$  are obtained for mass velocity  $G=35\text{kg/m}^2\text{s}$  ( $V_{in,total} = 0.95\text{ l/min}$ ) at  $s=5\text{mm}$  and for  $G=79\text{kg/m}^2\text{s}$  ( $V_{in,total} = 1.7\text{ l/min}$ ) at  $s=2\text{mm}$ , where the mass velocities are calculated by hypothetical inlet liquid velocities under the assumption that the total flow rate is distributed uniformly to both of heated and unheated channels. As far as the same mass velocities are concerned, the CHF values in the present experiment are far larger than those predicted by Katto-Kurata correlation for  $L=150\text{ mm}$  (interpolated values between those for  $L=30\text{mm}$  and  $L=300\text{mm}$  in Fig.2(b)).

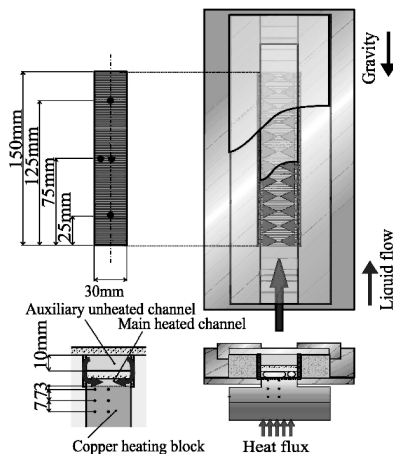


Fig. 11 A structure of narrow heated channel assembly with auxiliary liquid supply.

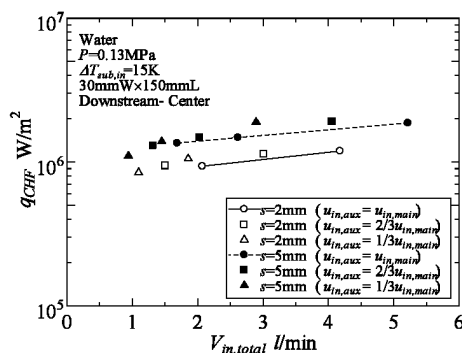


Fig. 12 Relation between values of CHF and total volumetric flow rate for a heating surface with a heated length of 150mm.

## 6. Conclusions

Feasibility of the bulk laser type SSPS is examined from a view of thermal management by using two-phase fluid flow, where the cooling medium is flowing in rectangular channels attached directly to the laser medium. The possibility of cooling by two-phase fluid flow is discussed in terms of critical heat flux and temperature distribution in the laser medium.

- i) Critical heat flux increases with increase in mass velocity, channel height, or saturation temperature, while it decreases with heated length.
- ii) When water is used, critical heat flux can be higher than estimated heat flux on the surface of the laser medium, while this is not true for cooling by FC72.
- iii) The temperature of the surface where laser beam enters becomes extremely high because of the temperature difference required for the thermal conduction across the laser medium. To maintain this temperature at lower levels, the ranges in the selection of fluid saturation temperature, laser materials and thickness of the laser medium is quite limited.
- iv) Under microgravity conditions, more detailed examination is required for the determination of the channel dimensions and fluid flow conditions based on the reliable database of critical heat flux and heat transfer.
- v) To realize the high heat flux cooling from a large area, the new structure of narrow channel is devised. In the experiment, CHF values larger than  $1 \times 10^6 \text{W/m}^2$  are obtained for the heating surface with a length of 150mm.

## References

- 1) Ando, M., Kawasaki, H., Inoue, K., Shinmoto, Y., and Ohta, H., Feasibility Study on Two-phase Thermal Management Systems for Space Solar Power Satellite, *J. Jpn. Soc. Microgravity Appl.* **21**, 37, 2004
- 2) Ohta, H. et al., Feasibility Study on Waste Heat Management for Space Solar Power System, *SME Thermal Engineering Joint Conf.*, CD-ROM, 2003
- 3) Ohta, H., Ando, M., and Shinmoto, Y., Feasibility Study on the Thermal Management System for Space Solar Power System, *56<sup>th</sup> International Astronautical Congress*, CD-ROM, 2005
- 4) Katto, Y. and Kurata, C., Critical Heat Flux of Saturated Convective Boiling on Uniformly Heated Plates in a Parallel Flow, *Int. J. Multiphase Flow*, **6**, 575-582, 1980.
- 5) Mishima, K. and Ishii, M., Critical heat flux experiments under low flow conditions in a vertical annulus, ANL-82-6, NUREG/CR-2647, 1982.

Received October 25, 2006

Accepted for publication, July 13, 2007